https://doi.org/10.33472/AFJBS.6.6.2024.8159-8167

African Journal of Biological Sciences

Journal homepage: http://www.afjbs.com

Research Paper Open Access

Medical Image Denoising in Compound Noise Based on Convolution Neural Networks

Vishal Rajendrabhai Patel[1], Dr. Ronak Kumar Patel[2]

[1]Research Scholar, Departmentof Computerscience, Sankalchand Patel University, Visnagar, Gujarat, India.
[2]Associate Professor, Shrimad Rajchanddra Institute of Management and Computer Application, Uka Tarsadia University, Bardoli, Gujarat, India.

Article Info

Volume 6, Issue 6, August 2024

Received: 11 June 2024

Accepted: 14 July 2024

Published: 09 August 2024

doi: 10.33472/AFJBS.6.6.2024.8159-8167

ABSTRACT:

A medical imaging technique used for illness diagnosis and screening is low dose X-ray imaging. Unfortunately, mechanical noise makes it difficult to analyze such images. Despite significant advancements, some deep learning-based denoising methods still perform poorly on actual X-ray pictures. Due to the complexity of the X-ray image's actual noise. In order to replicate the true X-ray image, we create a noise model in this study based on the basic principles of X-ray imaging. Our proposal for improving low-dose X-ray images is to use a Blind Denoising Convolutional-Neural-Network (BDCNN). The experimental findings demonstrate that BDCNN outperforms the other denoising techniques in terms of denoising performance.

Keywords: X-ray, denoising, CNN

1. INTRODUCTION

An essential medical imaging technique for diagnosing conditions like tuberculosis, pneumonia, bone fractures, congestive heart failure, and stones is X-ray imaging. Nevertheless, different kinds and intensities of noise throughout the imaging phase and transmission taint the quality of X-ray images. The analysis, diagnosis, and treatment of illnesses are all adversely impacted by the tainted X-ray pictures. As a result, improving the caliber of X-ray images is essential. There are two primary approaches to achieving this objective. One is extending the X-ray's radiation exposure duration or dosage.
The other approach involves using image de-noising methods to enhance the accuracy of the X-ray images. Recent studies have shown that this approach will increase certain risks associated with high radiation dosages or frequent exposures to radiation, such as the risk of developing cancer [1]. Still, decreasing incident photon density and photon unevenness under low radiation dosages will result in a much higher quantum noise (also known as shot noise, photon noise, or Poisson noise), which is a signal-dependent noise [2]. To improve the quality of X-ray images, image denoising methods have been developed for many years. Several image denoising techniques, including block matching and 3D filtering (BM3D) [3], non-local means [4], and total variation regularized approach [5], were used in the early years to reduce the noise in X-ray images.

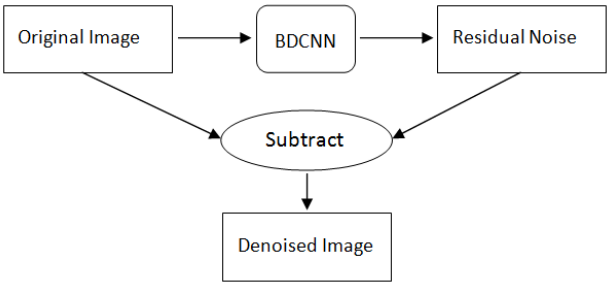

Figure 1: Overview of the proposed method. BDCNN takes the noisy X-ray image as the input and outputs the corresponding residual noise map. The final denoised image is the difference between the input noisy X-ray image and the residual noise map.
Based on the properties of X-ray imaging networks, signal-related quantum noise is more influential on images than thermal noise. Photon-limited imaging systems can enhance their image quality by employing a Poisson non-local principle component analysis approach [6] to counteract Poisson noise. One efficient technique for Poisson noise, as demonstrated by [1,10], is the variance stabilizing transform (VST) method. Poisson noise is first converted by VST into a signal-independent Gaussian noise form, after which the noise can be reduced using Gaussian noise denoising techniques. Inverse VST will yield the final restored image. For X-ray images, VST-based denoising techniques are more appropriate than those suggested for Gaussian noise. Nevertheless, there is still room for improvement because the VST-based approaches do not account for the Gaussian noise present in X-ray images.
This work suggests a blind denoising technique for X-ray images based on CNN (BDCNN) to guarantee the high-quality efficiency of noise reduction. The proposed BDCNN receives the noisy X-ray image as input and produces the matching residual noise map, as seen in Figure 2. The residual noise maps can be subtracted from the noisy image to produce the final denoised picture. Two sub networks make up BDCNN: one for noisy level estimation (NLE) and the other for non-blind denoising (NBD). The NBD sub network will receive the predicted noise levels that the NLE sub network determines from the input X-ray pictures. We employ a more appropriate noise model in line with X-ray imaging systems to synthesize

the training data, since the distribution of synthetic noisy X-ray images will greatly impact the training of deep learning-based denoising algorithms.

2. RELATED WORKS

2.1 CNN based denoising methods

Image denoising has significantly improved in performance. Zhang et al. [7] recommended a denoising method based on deep CNNs for image denoising, which has greater denoising performance than conventional image denoising methods. Zhang et al. [8] proposed a fast and flexible CNN based model FFDNet. as FFDNet [8] uses an additional noise level map as input, that may eliminate noise from noisy images, which have spatially variant noise and an extensive variety of noise levels. In [9], a two phase model CBDNet was suggested to handle noisy photographs in real-world scenarios.

Image denoising has significantly improved in performance. Zhang et al. [7] recommended a denoising method based on deep CNNs for image denoising, which has greater denoising performance than conventional image denoising methods. Zhang et al. [8] proposed a quick and adaptable CNN based model FFDNet. as FFDNet [8] uses an additional noise level map as input, that may eliminate noise from noisy images, which have spatially variant noise and an extensive variety of noise levels. In [9], a two phase model CBDNet was suggested to handle noisy photographs in real-world scenarios. DNet [9] is capable of handling noisy images with varying noise levels by retraining its subnetwork to calculate the noise level. For the purpose of denoising X-ray images, the convolutional encoder decoder network SkiDNet was introduced in [10]. A CNN-based denoising model for X-ray pictures, called X-ReCNN, was proposed by Jin et al. [11] employing a depth-wise separable convolution and the residual learning technique.

The majority of the aforementioned techniques address noisy photos by creating realistic noise models that accurately reflect the noise and strong network designs. Network architectures can be designed using a variety of techniques, including adding skip connections or batch normalization operations [14, 24] into the network architectures, modifying the loss function [6, 9], adding additional information for CNN [9, 28], increasing the CNN's depth or width, and implementing residual learning strategy [8, 14, 27]. In this study, we combine the best features of existing CNN-based techniques to propose a novel denoising model for X-ray images, called XBDCNN.

2.2 Image noise modeling

To train their model, the majority of deep learning-based picture denoising techniques require clean-noise pairs. There aren't many actual noisy photographs, though, nor matching clean images. Consequently, creating training samples using an image noise model is a common technique. AWGN, or addition white Gaussian noise, is a popular technique for producing training data.

The actual noisy image's noise is complex and varied, not entirely following the Gaussian distribution. As a result, when applied to actual noisy photos, the CNN-based denoising technique that was trained on Gaussian noisy images performs poorly. To train SkiDNet using three distinct forms of noisy X-ray images—Gaussian noise, Salt and Pepper noise, and Poisson noise—Dutta et al. [10] used a variety of noisy X-ray image types. But because the basic principle underlying noisy X-ray images is disregarded, these artificial noisy X-ray photos do not resemble true noisy X-ray images.

It is well knowledge that training data plays a major role in how well CNN-based denoising techniques perform. For X-ray images to perform better when denoising, a more accurate noise model needs to be created.

2.3 Blind de-noising

For noisy images with unknown noise kinds or unknown noise intensities, blind denoising techniques are developed [12]. Because various forms of noise in the actual world can readily contaminate recorded images, and the amount of such noise is frequently unknown. Therefore, developing picture blind denoising technology is crucial. Noise estimation and non-blind denoising are two processes that are frequently included in blind denoising. A PCA-based approach to estimate the noise standard deviation for AWGN was proposed by Chen et al. [13]. In order to eliminate noise, Zhang et al. [8] presented FFDNet, which uses the noise level map—that is, the noise standard deviation—as additional information from CNN. The noise level must be manually adjusted with FFDNet, though. Later on, Guo and colleagues. [9] put forth the CBDNet blind denoising technique. To estimate the noise level map, it initially employs CNN. To obtain the denoised image, the estimated noise level map is then fed into a non-blind denoising subnetwork.

It is more difficult for blind denoising to minimize noise than non-blind denoising because of unknown noise types and intensities. Thus, measuring the noise level is an excellent way to convert a blind denoising problem to a non-blind denoising problem.

3. PROPOSED METHOD

3.1 Compound gaussian-poisson noise model

The majority of techniques for denoising X-ray images are trained on noisy images including either Poisson or Gaussian noise. Nevertheless, these techniques typically perform poorly on actual noisy X-ray pictures. To produce training samples, a more accurate noise model for X-ray pictures must be constructed.

X-ray imaging systems typically experience two kinds of noise, as stated in [14]: thermal noise, which is unrelated to signals, and quantum noise, which is related to signals. In order to replicate the deterioration process of low-dose X-ray images, we construct a hybrid Poisson-Gaussian noise model based on this feature, which is defined as

$$Y = Xp + N$$

where N is the thermal noise, which is a signal-independent Gaussian noise with zero-mean and variance $\sigma 2$, X is the image damaged by Poisson noise, Y is the noisy image, and X is the given clean X-ray image.

The various parts of the human body absorb X-rays to varying degrees, which is the fundamental basis of X-ray imaging. The photons' energy is reduced and their direction of scattering is altered due to the Compton effect [11], resulting in X-ray images that are contaminated with quantum noise.

3.2 CNN based denoising method

The noise level σ and η, respectively, determine the intensity of Gaussian and Poisson noise in X-ray pictures, according to the hybrid Poisson-Gaussian noise model. Naturally, the quality of the denoised image from the noisy original image is enhanced by the known noise levels, σ and η. Driven by this, we suggest a new neural network, called X-BDCNN, for denoising X-ray images. The NLE and NBD sub networks are its two constituent sub

networks. To estimate the noise level map, the noisy X-ray pictures Y are sent into the NLE sub network. We make the noise level map the same width and height as the noisy image input for ease.

3.3 Evaluation metric

We employ three standard picture quality evaluation techniques to compare the quality of the denoised image produced by various denoising techniques in order to quantitatively assess the denoising image's performance.

1) Signal to noise (SNR): The signal-to-noise ratio, or SNR, is calculated. Measuring the disparity between the ground truth image and the denoised image is another application for it. It is defined as

$$\mathrm{SNR}\left(X,\hat{X}\right)=10\log_{10}\frac{\sum_{x\in\Omega}|\hat{X}(x)|^2}{\sum_{x\in\Omega}\left|X(x)-\hat{X}(x)\right|^2},$$

2) **Peak Signal Noise Ratio (PSNR):** Based on the difference in corresponding pixels between the denoised image and the ground truth image, PSNR is the most popular and extensively used objective image evaluation technique. The mathematical formula is given by

$$\mathrm{PSNR}(X,\hat{X})=10\log_{10}\frac{MAX_X^2}{\frac{1}{\Omega}\sum_{x\in\Omega}|X(x)-\hat{X}(x)|^2},$$

The higher the value of the three image quality evaluation techniques mentioned above, the higher the quality of the denoised image in the context of image restoration. This indicates that the matching denoising technique performs better.

4. EXPERIMENTS AND RESULTS

4.1 Experimental setting

Training and Testing Data: 108,948 kidney X-ray images are part of the public kidney X-ray collection Kidney X-ray8 [15]. It contains 1024 × 1024 images, all of which are of excellent visual quality and free of noise.

From this collection, 1000 X-ray pictures were chosen at random and cropped into 128 × 128 patches. In total, we collected 32000 patches, which we divided into three sets: a training set, a validation set, and a test set, with a 7:2:1 ratio. Several artificial noisy X-ray images were created in accordance with the compound Gaussian-poison noise model detailed in section 3.1 in order to train our algorithm.

4.2 Compared methods

We selected three cutting-edge denoising techniques—BM3D [16], DnCNN [7], and X-ReCNN [17] - to compare with BDCNN in order to assess the effectiveness of the suggested approach. Although it takes a while, the non-local similarity based BM3D technique can handle noisy images with different levels of noise. The final two techniques rely on CNN. One helpful model for image denoising is DnCNN [7]. With the exception of the noise model, we ran our experiments using the author's code and default parameter settings. A proposed method for denoising X-ray images is X-ReCNN [17].

4.3 Analyze for proposed noise model

In Section 3.1, a Compound Gaussian-Poisson noise model is constructed to replicate noisy X-ray images obtained with low dosage X-ray radiation. Since Gaussian noise is independent of the signal and positively correlated with the noise level σ, we concentrate on analyzing low dosage X-ray images using Poisson noise. Finally, we suggest a Compound Gaussian-Poisson noise model to mimic noisy images based on the X-ray imaging physical basis. The X-ray pictures' Gaussian and Poisson noise intensities are adjusted, respectively, by the parameters σ and η. In X-ray pictures, a larger σ indicates more Gaussian noise and a larger η indicates less Poisson noise. Through experiments, we determine the appropriate values of $\sigma \in (0, 20)$ and $\eta \in (0.4, 1.8)$ for modeling noisy X-ray pictures.

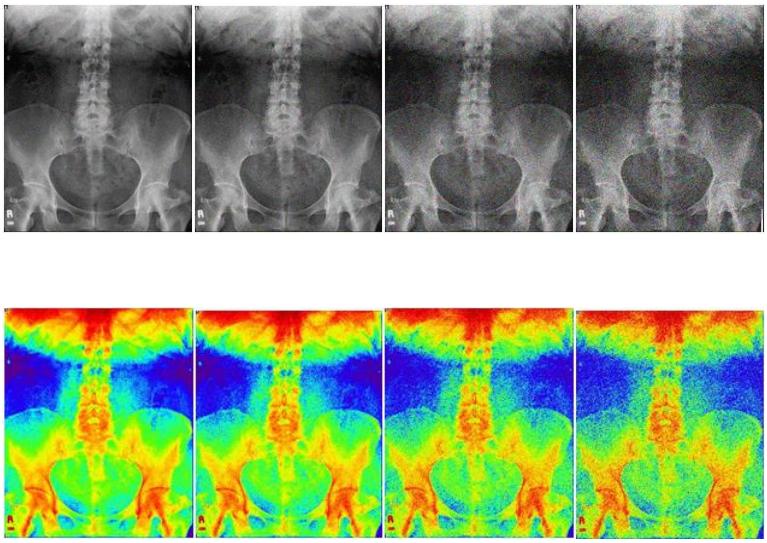

(a)

(b)

Figure 2: Analysis of Poisson noise. (a) The noisy images corrupted by the Poisson noise with different scale factors η. The first column is the clean image, and the second column to the last column is the corresponding noisy images with different scale factors (η=0.4, 0.6, 0.8), respectively. (b) The heatmap of residual noise images. From left to right is the residual noise images between different Poisson noise images and the same clean image with the scale factors η = 0.4, 0.6, 0.8, 1.0, respectively.

Table 1 compares the average SNR, PSNR, and SSIM values obtained from the CheX-ray8 dataset Test set using several denoising techniques [25].

Methods	SNR	PSNR	SSIM	Time (s)
Before Denoising	18.8836	24.1916	0.5100	---------
BM3D [3]	29.2848	34.5929	0.8639	0.152
DnCNN [7]	35.3720	40.3754	0.9822	0.005
X-ReCNN [17]	33.5900	38.4869	0.9740	0.004
X-BDCNN	36.1196	41.1070	0.9838	0.006

4.4 Qualitative evaluation on real x-ray images

We conduct tests on a number of actual noisy X-ray images of CheXpert in order to confirm the efficacy of X-BDCNN [18]. Figure 5 shows the denoising results produced by our X-BDCNN, XReCNN [17], and DnCNN [7]. It was noticed that while X-ReCNN [17] removed noise, the X-ray images suffered from blur effect and loss of features. On the other hand, alternative techniques could prevent the blur effect and eliminate noise. It is observed that the

three CNN-based denoising techniques are able to reduce noise and enhance image quality. This could be because the training data produced by our suggested hybrid noise model resembles the genuine noisy X-ray images. The issue of oversmoothing in denoised X-ray images has also been identified in [19], and they think it is challenging to prevent oversmoothing in denoised X-ray images while de-noising them.

4.5 Disease identification performance

The best way to assess the quality of X-ray images denoised using various techniques is to look at the accuracy of disease diagnosis based on X-ray images. However, diagnosing an illness from thousands of X-ray images takes a long time for doctors, and their expertise and experience have an impact on the diagnosis of X-ray images. Therefore, in order to compare the quality of X-ray pictures denoised by various approaches, we select the illness classification method CIA-Net [20]. Based on a chest X-ray image, CIA-Net can classify 14 different diseases and reach state-of-the-art classification results [20]. The AUC (Area under the Curve) scores for each of the 14 illness classifications on the 1000 X-ray pictures that were denoised using various techniques. The results show that the genuine noise-free X-ray images have the highest mean AUC score, whereas the synthetic noisy X-ray images have the lowest mean AUC score.

It is demonstrated that, in most situations, the AUC scores on X-BDCNN are lower than those on the original, noise-free X-ray pictures. X-ray image denoised by X-BDCNN has a lower quality than the original noise-free image; however, this difference is not as great as that of noisy X-ray images. Table 6's "Fibrosis" and "Nodule" columns indicate an anomalous situation in which two kinds of diseases had higher AUC scores on the synthetic noisy X-ray pictures than on the other images. The two disease types may be difficult to distinguish, and noise interference makes it more likely that they will be correctly identified.

5. CONCLUSIONS

Although low-dose X-ray imaging frequently involves noise, it poses less risk to humans. To enhance the standard of X-ray images, we have therefore suggested the X-BDCNN X-ray image denoising approach. In order to ensure that X-BDCNN can be applied to actual noisy X-ray scans, we combine the physical principles of low-dose X-ray imaging with a compound Poisson-Gaussian noise model. The NLE subnetwork's estimated noise level is used to help the NBD subnetwork perform better at denoising. Furthermore, the SSIM is used into a loss function for training X-BDCNN in order to ensure the structural information of denoised an X-ray picture. Numerous tests on artificial and real-world noisy X-ray pictures have shown that BDCNN performs better in terms of qualitative as well as quantitative quality assessments. The outcome of the disease identification process confirms our method's efficacy even further. BDCNN is applicable to various medical pictures related to X-ray imaging, such as computed tomographic scans, even though we only assess its performance on X-ray images. It is noteworthy to mention that the true noise model of low-dose X-ray images, that is challenging to characterize in practice, can differ slightly from our suggested compound Poisson-Gaussian noise model. Training data for deep learning-based denoising techniques should be produced by investigating a more precise noise simulation of low dose X-ray images.

6. REFERENCES

1. [1] Rebecca Smith-Bindman, Jafi Lipson, Ralph Marcus, Kwang-Pyo Kim, Mahadevappa Mahesh, Robert Gould, Amy Berrington De González, and Diana L Miglioretti. 2009. Radiation dose associated with common computed tomography examinations and the associated lifetime attributable risk of cancer. Archives of internal medicine 169, 22 (2009), 2078–2086.
2. Mario Cesarelli, Paolo Bifulco, Tommaso Cerciello, Maria Romano, and Luigi Paura. 2013. X-ray fluoroscopy noise modeling for filter design. International journal of computer assisted radiology and surgery 8, 2(2013), 269–278.
3. Kostadin Dabov, Alessandro Foi, Vladimir Katkovnik, and Karen Egiazarian. 2007. Image denoising by sparse 3-D transform-domain collaborative filtering. IEEE Transactions on image processing 16, 8 (2007), 2080–2095.
4. Antoni Buades, Bartomeu Coll, and J-M Morel. 2005. A non-local algorithm for image denoising. In 2005 IEEE Computer Society Conference on Computer Vision and Pattern Recognition (CVPR'05), Vol. 2. IEEE, 60–65.
5. Leonid I Rudin, Stanley Osher, and Emad Fatemi. 1992. Nonlinear total variation based noise removal algorithms. Physica D: nonlinear phenomena 60, 1-4 (1992), 259–268.
6. Joseph Salmon, Zachary Harmany, Charles-Alban Deledalle, and Rebecca Willett. 2014. Poisson noise reduction with non-local PCA. Journal of mathematical imaging and vision 48, 2 (2014), 279–294.
7. Kai Zhang, Wangmeng Zuo, Yunjin Chen, Deyu Meng, and Lei Zhang. 2017. Beyond a gaussian denoiser: Residual learning of deep cnn for image denoising. IEEE Transactions on Image Processing 26, 7 (2017), 3142–3155.
8. Kai Zhang, Wangmeng Zuo, and Lei Zhang. 2018. FFDNet: Toward a fast and flexible solution for CNN-based image denoising. IEEE Transactions on Image Processing 27, 9 (2018), 4608–4622.
9. Shi Guo, Zifei Yan, Kai Zhang, Wangmeng Zuo, and Lei Zhang. 2019. Toward convolutional blind denoising of real photographs. In Proceedings of the IEEE Conference on Computer Vision and Pattern Recognition. 1712–1722.
10. Sandipan Dutta, Shaurya Chaturvedi, Swaraj Kumar, and MPS Bhatia. 2019. SkiDNet: Skip Image Denoising Network for X-Rays. In 2019 International Joint Conference on Neural Networks (IJCNN). IEEE, 1–8.
11. G Harding, H Strecker, and R Tischler. 1983. X-ray imaging with Compton-scatter radiation. Philips technical review 41, 2 (1983), 46–59.
12. Chunwei Tian, Lunke Fei, Wenxian Zheng, Yong Xu, Wangmeng Zuo, and Chia-Wen Lin. 2020. Deep learning on image denoising: An overview. Neural Networks (2020).
13. Guangyong Chen, Fengyuan Zhu, and Pheng Ann Heng. 2015. An efficient statistical method for image noise level estimation. In Proceedings of the IEEE International Conference on Computer Vision. 477–485.
14. Tej Bahadur Chandra and Kesari Verma. 2020. Analysis of quantum noise-reducing filters on chest X-ray images: A review. Measurement 153(2020), 107426.
15. Xiaosong Wang, Yifan Peng, Le Lu, Zhiyong Lu, Mohammadhadi Bagheri, and Ronald M. Summers. 2017. ChestX-ray8: Hospital-Scale Chest X-Ray Database and Benchmarks on Weakly-Supervised Classification and Localization of Common Thorax Diseases. In Proceedings of the IEEE Conference on Computer Vision and Pattern Recognition (CVPR).
16. Kostadin Dabov, Alessandro Foi, Vladimir Katkovnik, and Karen Egiazarian. 2007. Image denoising by sparse 3-D transform-domain collaborative filtering. IEEE Transactions on image processing 16, 8 (2007), 2080–2095.

17. Yan Jin, Xiao-Ben Jiang, Zhen-kun Wei, and Yuan Li. 2019. Chest x-ray image denoising method based on deep convolution neural network. IET Image Processing 13, 11 (2019), 1970–1978.
18. Jeremy Irvin, Pranav Rajpurkar, Michael Ko, Yifan Yu, Silviana Ciurea-Ilcus, Chris Chute, Henrik Marklund, Behzad Haghgoo, Robyn Ball, Katie Shpanskaya, et al. 2019. Chexpert: A large chest radiograph dataset with uncertainty labels and expert comparison. In Proceedings of the AAAI Conference on Artificial Intelligence, Vol. 33. 590–597.
19. Yimin Luo, Sophie Majoe, Kui Jiang, Haikun Qi, Kuberan Pushparajah, and Kawal Rhode. 2020. Ultra-Dense Denoising Network: Application to Cardiac Catheter-based X-ray Procedures. IEEE Transactions on Biomedical Engineering(2020).
20. Jingyu Liu, Gangming Zhao, Yu Fei, Ming Zhang, Yizhou Wang, and Yizhou Yu. 2019. Align, attend and locate: Chest x-ray diagnosis via contrast induced attention network with limited supervision. In Proceedings of the IEEE/CVF International Conference on Computer Vision. 10632–10641.